Journal of Molecular Spectroscopy 325 (2016) 35–41

Contents lists available at ScienceDirect

Journal of Molecular Spectroscopy

journal homepage: www.elsevier.com/locate/jms

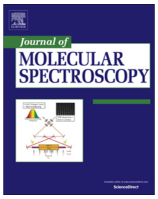

Observation and analysis of the SF_6 $\nu_2 + \nu_4 - \nu_5$ band: Improved parameters for the $v_5 = 1$ state

M. Faye [a], V. Boudon [b], M. Loëte [b], P. Roy [a], L. Manceron [a,c,*]

[a] Ligne AILES – Synchrotron SOLEIL, L'Orme des Merisiers, F-91192 Gif-sur-Yvette, France
[b] Laboratoire Interdisciplinaire Carnot de Bourgogne, UMR 6303 CNRS-Université de Bourgogne Franche-Comté, 9 Av. A. Savary, BP 47870, F-21078 Dijon Cedex, France
[c] Laboratoire MONARIS, CNRS UMR 8233, 4 Place Jussieu, F-75252 Paris Cedex, France

ARTICLE INFO

Article history:
Received 7 April 2016
In revised form 7 June 2016
Accepted 7 June 2016
Available online 9 June 2016

Keywords:
Rotation–vibration spectroscopy of SF_6
Greenhouse gas
Hot band
Infrared absorption
Tensorial formalism
Long-path cell
Low temperature

ABSTRACT

In this paper, we present the high resolution analysis of the weak $\nu_2 + \nu_4 - \nu_5$ band of SF_6 around 735 cm^{-1}. The spectra were recorded on the AILES Beamline at the SOLEIL Synchrotron facility using a cryogenic multipass cell coupled to a Bruker 125HR spectrometer with a maximum resolution of 0.00102 cm^{-1}. For this band, we worked with 4 mbar of SF_6 at a temperature of 223 ± 2 K. The optical path length was fixed to 141 m and the spectrum recorded with 0.001 cm^{-1} of resolution. A new, cold spectrum of the $\nu_2 + \nu_4$ band was also collected at 153 K, 15-m path length, and 0.0015 cm^{-1} resolution. The analysis was performed by using the Dijon group XTDS and SPVIEW software, based on tensorial formalism. We achieved correct simulation and line position assignments of the $\nu_2 + \nu_4 - \nu_5$ band, by gathering $\nu_2 + \nu_4$ data and ν_5 Raman data. We could assign 3553 transition for $\nu_2 + \nu_4 - \nu_5$ with a standard deviation of 1.292×10^{-3} cm^{-1}. This analysis also helped improve the $v_2 = v_4 = 1$ level and the $v_5 = 1$ fundamental level $v_2 = v_4 = 1$.

1. Introduction

The rotation–vibration spectroscopy of SF_6, as a prototypical molecule for metal hexafluorides of great practical interest, has generated a substantial body of work (see Refs. [1–4] and references therein). The well-known infrared (IR) and Raman strongly active fundamentals ν_1–ν_4 have been measured and analyzed to a great level of precision in Refs. [5–10]. Nevertheless, due to the complexity of the problems and the particular properties of O_h symmetry molecules, some important data were missing until recently, or are still missing.

With the development of new setups using synchrotron radiation (SR)-based instrumentation, new perspectives have recently opened: until a recent study [11], the lowest mode, ν_6, neither permitted at first order in IR absorption nor in Raman measurements, had remained poorly known. Other issues remain; in particular, the modeling of the many hot bands in the ν_3 region, of interest for atmospheric detection, has posed a particular problem: many transitions are overlapping and a direct rovibrational analysis is impossible [4]. A possible strategy involves observation of combination bands accessing the transition upper levels, but these transitions are not always active or intense enough to be useful. An alternative route involves observation of difference bands, which proved useful for modeling the weak $\nu_3 + \nu_1 - \nu_1$ or $\nu_3 + \nu_2 - \nu_2$ [12]. To access the main hot band, $\nu_3 + \nu_6 - \nu_6$, a comparable strategy imposes to seek a band with a common upper level, the only possibility being thus $\nu_3 + \nu_6 - \nu_4$. This very weak band is in the neighborhood of other low-frequency transitions, $2\nu_5 - \nu_6$ and $\nu_2 + \nu_4 - \nu_5$, but as they have no common upper or lower levels, they do not interact and can be modeled separately.

Our aim in this study is thus a stepwise analysis of this region to finally access the $v_3 = v_6 = 1$ level parameters. These transitions are located below 800 cm^{-1}, and their location and their weak activity makes them challenging for high-resolution spectroscopic techniques. For practical reasons, the first step was an analysis of the $\nu_2 + \nu_4 - \nu_5$ transition to disentangle the end of its *P* branch from the beginning of the *R* branch of the next band. The upper level corresponds to $v_2 = v_4 = 1$, and a previous analysis of the $\nu_2 + \nu_4$ combination [9] provides the necessary starting point. The ν_5 mode (of F_{2g} symmetry) has been the object of a high-resolution, stimulated Raman investigation [13]. However, due to technical difficulties, only the *Q*, *R*, and *S* branches could be observed, thus making the ν_5 band parameters perhaps the less precisely determined of all SF_6 fundamentals. Indeed, in the course of our study, it was found that the available parameters could not lead to a satisfactory modeling of the $\nu_2 + \nu_4 - \nu_5$ difference band.

---

* Corresponding author at: Ligne AILES – Synchrotron SOLEIL, L'Orme des Merisiers, F-91192 Gif-sur-Yvette, France.

E-mail address: laurent.manceron@synchrotron-soleil.fr (L. Manceron).

http://dx.doi.org/10.1016/j.jms.2016.06.003
0022-2852/

New data recorded here at 223 and 153 K at higher resolution (0.001 cm^{-1}) were used, together with former assignments and line list, to refine both $v_5 = 1$ and $v_2 = v_4 = 1$ level parameters, which is the objective of the present paper.

2. Experiment

Because of the expected weakness of the induced IR activity of the $\nu_2 + \nu_4 - \nu_5$ region and to help simplify the analysis, a high signal-to-noise and a long optical path length at low temperature were required. A high-resolution spectrum was recorded on the AILES Beamline at Synchrotron SOLEIL on the Synchrotron light source coupled to a Bruker 125HR interferometer [14,15] using the newly developed cryogenic multipass cell, set on a 141-m optical path length and regulated at a temperature of 223 ± 2 K along the entire optical path. For the $\nu_2 + \nu_4$ region, the path length was reduced to 15 m and the temperature to 153 K. This setup has been fully described elsewhere [16]; only a few relevant details will be given here. The cell optical setup is based on a Barskaya–Chernin five-mirror arrangement with a 1.5-m base length [17], providing for maximum vibrostability, and on electrically driven micrometer opto-mechanical supports mounted on invar rods. The optical path length can be adjusted in 3-m increments between 3 and 141 m in the far IR, but longer path lengths can be achieved in the near-IR to mid-IR. The mirrors can be retuned at any time and the optical path rechecked with a coaxial laser beam that was visible. The cell is mounted inside a triple-jackets liquid nitrogen cryostat. The cooling power from a liquid nitrogen-filled surrounding envelope is transmitted by an annular space filled by helium as convection gas, and its pressure can be varied to adjust the cooling power. Additional heaters are distributed along the gas cell body for a fine adjustment and temperature homogenization. The cell and the outside Dewar jacket are fitted with diamond windows brazed on stainless steel flanges to enable operation of the cell between 80 and 400 K from the near IR to the THz range. To limit acoustic noise, once in operation, only vibration-free ionic and cryogenic traps are used. Two spectra were used here. For the $\nu_2 + \nu_4$ region, a spectrum with a 15-m optical path length, 153 K temperature, and a gas pressure of 0.09 mbar of SF$_6$ (Air Liquide, France, 99.9% purity) was recorded at 0.0015 cm^{-1} resolution in the 1800–900 cm^{-1} region, using the globar internal source, averaging 1426 scans in about 36 h. No apodization was applied (boxcar software option) and a 5.06-cm/s scanner velocity, a Ge/KBr beamsplitter, and a D316 Infrared associates HgCdTe with 30° field stop were used. For the $\nu_2 + \nu_4 - \nu_5$ region, a 141-m path length with a cell temperature of 223 K and a higher, 4-mb gas pressure were chosen. The Soleil SR operating at a ring current of 430 mA was used as a source. A special, 4 K-cooled homemade HgCdTe photoconductive detector equipped with a cold, 930 cm^{-1} low-pass filter and dedicated electronics was used, achieving an eightfold increase in signal-to-noise ratio versus commercially available detectors in this region for HR measurements. This equipment will be described elsewhere [18]. Then, 2366 interferograms were averaged in a total recording time of about 94 h and processed against a background of the empty cell taken at the same temperature at a resolution of 0.01 cm^{-1}. Spectra were zero-filled, corrected for channelling effects, and calibrated using well-known carbonyl sulfide and carbon dioxide lines [19].

3. Theoretical model

In this paper, we use the theoretical model based on tensorial formalism and the vibrational extrapolation developed by the Dijon group [20]. The principles of this model are explained in brief, as they have already been detailed in Ref. [21]. Considering an XY$_6$ molecule as SF$_6$, the vibrational levels are grouped in a series of polyads designated as P_k with $k = 0, \ldots, n$. For $k = 0$, we have P_0, which is the ground state (GS). The Hamiltonian operator is written as follows:

$$\mathcal{H} = \mathcal{H}_{\{P_0 \equiv GS\}} + \mathcal{H}_{\{P_1\}} + \cdots + \mathcal{H}_{\{P_k\}} + \cdots + \mathcal{H}_{\{P_{n-1}\}} + \mathcal{H}_{\{P_n\}}. \tag{1}$$

where the different $\mathcal{H}_{\{P_k\}}$ terms are expressed in the following form:

$$\mathcal{H}_{\{P_k\}} = \sum_{\text{all indexes}} t_{\{s\}\{s'\}}^{\Omega(K,n\Gamma)\Gamma_v\Gamma'_v} \beta \left[{}^{\varepsilon}V_{\{s\}\{s'\}}^{\Omega_v(\Gamma_v\Gamma'_v)\Gamma} \otimes R^{\Omega(K,n\Gamma)} \right]^{(A_{1g})}. \tag{2}$$

In Eq. (2), $t^{\Omega(K,n\Gamma)\Gamma v\Gamma' v}$ are the parameters to be determined, whereas ${}^{\varepsilon}V_{\{s\}\{s'\}}^{\Omega_v(\Gamma_v\Gamma'_v)\Gamma}$ and $R^{\Omega(K,n\Gamma)}$ are vibrational and rotational operators, respectively, and of respective degree Ωv and Ω. β is a factor that allows the scalar terms ($\Gamma = A_{1g}$) to match the usual terms such as $B_0 J^2$. The order of each individual term is defined as $\Omega + \Omega_v - 2$.

In this model, we deal with an effective Hamiltonian that is obtained, for a given polyad P_k, by the projection of H in the P_n Hilbert subspace, as in Eq. (3):

$$H^{\langle P_n \rangle} = P^{\langle P_n \rangle} \mathcal{H} P^{\langle P_n \rangle} = H_{\{GS\}}^{\langle P_n \rangle} + H_{\{P_1\}}^{\langle P_n \rangle} + \cdots + H_{\{P_k\}}^{\langle P_n \rangle} + \cdots + H_{\{P_{n-1}\}}^{\langle P_n \rangle} + H_{\{P_n\}}^{\langle P_n \rangle}. \tag{3}$$

Thus, we can write the effective Hamiltonian of each polyad involved in the study of any band. In the case of $\nu_2 + \nu_4 - \nu_5$, all the effective Hamiltonian operators must include terms relative to all states involved in the difference band, and are thus as follows:

- For the ground state,

$$H^{\langle GS \rangle} = H_{\{GS\}}^{\langle GS \rangle} \tag{4}$$

- For the $v_5 = 1$ level,

$$H^{\langle P_1 = \nu_5 \rangle} = H_{\{GS\}}^{\langle P_1 = \nu_5 \rangle} + H_{\{P_1 = \nu_5\}}^{\langle P_1 = \nu_5 \rangle} \tag{5}$$

- For the $v_4 = 1$ level,

$$H^{\langle P_2 = \nu_4 \rangle} = H_{\{GS\}}^{\langle P_2 = \nu_4 \rangle} + H_{\{P_1 = \nu_5\}}^{\langle P_2 = \nu_4 \rangle} + H_{\{P_2 = \nu_4\}}^{\langle P_2 = \nu_4 \rangle} \tag{6}$$

- For the $v_2 = 1$ level,

$$H^{\langle P_3 = \nu_2 \rangle} = H_{\{GS\}}^{\langle P_3 = \nu_2 \rangle} + H_{\{P_1 = \nu_5\}}^{\langle P_3 = \nu_2 \rangle} + H_{\{P_2 = \nu_4\}}^{\langle P_3 = \nu_2 \rangle} + H_{\{P_3 = \nu_2\}}^{\langle P_3 = \nu_2 \rangle} \tag{7}$$

- For the $v_4 = v_5 = 1$ level,

$$\begin{aligned} H^{\langle P_4 = \nu_4 + \nu_5 \rangle} = {} & H_{\{GS\}}^{\langle P_4 = \nu_4 + \nu_5 \rangle} + H_{\{P_1 = \nu_5\}}^{\langle P_4 = \nu_4 + \nu_5 \rangle} + H_{\{P_2 = \nu_4\}}^{\langle P_4 = \nu_4 + \nu_5 \rangle} \\ & + H_{\{P_3 = \nu_2\}}^{\langle P_4 = \nu_4 + \nu_5 \rangle} + H_{\{P_4 = \nu_4 + \nu_5\}}^{\langle P_4 = \nu_4 + \nu_5 \rangle} \end{aligned} \tag{8}$$

- For the $v_2 = v_5 = 1$ level,

$$H^{\langle P_5 = \nu_2 + \nu_5 \rangle} = H_{\{GS\}}^{\langle P_5 = \nu_2 + \nu_5 \rangle} + H_{\{P_1 = \nu_5\}}^{\langle P_5 = \nu_2 + \nu_5 \rangle} + H_{\{P_2 = \nu_4\}}^{\langle P_5 = \nu_2 + \nu_5 \rangle} + H_{\{P_3 = \nu_2\}}^{\langle P_5 = \nu_2 + \nu_5 \rangle} \tag{9}$$

$$+ H_{\{P_4 = \nu_4 + \nu_5\}}^{\langle P_5 = \nu_2 + \nu_5 \rangle} + H_{\{P_5 = \nu_2 + \nu_5\}}^{\langle P_5 = \nu_2 + \nu_5 \rangle} \tag{10}$$

- For the $v_2 = v_4 = 1$ level,

$$H^{\langle P_6 = \nu_2 + \nu_4 \rangle} = H_{\{GS\}}^{\langle P_6 = \nu_2 + \nu_4 \rangle} + H_{\{P_1 = \nu_5\}}^{\langle P_6 = \nu_2 + \nu_4 \rangle} + H_{\{P_2 = \nu_4\}}^{\langle P_6 = \nu_2 + \nu_4 \rangle} + H_{\{P_3 = \nu_2\}}^{\langle P_6 = \nu_2 + \nu_4 \rangle} \tag{11}$$

$$+ H_{\{P_4 = \nu_4 + \nu_5\}}^{\langle P_6 = \nu_2 + \nu_4 \rangle} + H_{\{P_5 = \nu_2 + \nu_5\}}^{\langle P_6 = \nu_2 + \nu_4 \rangle} + H_{\{P_6 = \nu_2 + \nu_4\}}^{\langle P_6 = \nu_2 + \nu_4 \rangle} \tag{12}$$

In this analysis, as we consider the transition from $v_5 = 1$ level to $v_2 = v_4 = 1$ level, the $\nu_4 + \nu_5$ and $\nu_2 + \nu_5$ effective Hamiltonian order of development is not relevant as it has no influence on the $\nu_2 + \nu_4 - \nu_5$ band behavior.

The calculation of the effective Hamiltonian matrix was performed on the coupled rovibrational basis: